

# **Report for 2004GA58B: Biogeochemical Cycling of Arsenic at the Sediment-Water Interface of the Chattahoochee River**

There are no reported publications resulting from this project.

Report Follows

# Biogeochemical Cycling of Arsenic at the Sediment-Water Interface of the Chattahoochee River

**Martial Taillefert**

School of Earth and Atmospheric Sciences  
Georgia Institute of Technology, Atlanta GA

May 16, 2005

## 1.0 Executive Summary

In a previous study, elevated dissolved arsenic concentrations were detected in the Chattahoochee River (GA) and decreased in concentration with increasing distance from a suspected point-source, suggesting that arsenic could be scavenged by particles and settle to the sediment-water interface (SWI). In this study, we investigated the cycling of arsenic in the sediment of the Chattahoochee River to determine if arsenic is accumulated in the sediment downstream from two coal-fire power plants and how arsenic is biogeochemically transformed in these sediments. To realize these objectives, a combination of state-of-the-art analytical techniques - ICP-MS and voltammetry - with other conventional techniques was used to determine, with a high spatial resolution, the distribution of arsenic between particulate and dissolved phase, the redox speciation of arsenic in the dissolved phase, and the distribution of other redox species ( $O_2$ ,  $SO_4^{2-}$ ,  $NO_3^-$ , Fe(II), Mn(II), and  $\Sigma H_2S$ ) in the first 10 centimeters of four sediment cores. Depth profiles suggest that iron oxides scavenge arsenic in the form of arsenate in the water column and settle to the SWI where they are reduced by iron reducing bacteria. As a result of microbial iron reduction, dissolved arsenic, in the form of As(V) only, is released and accumulates in the porewaters near the sediment-water interface, where it can diffuse back to the overlying waters, with fluxes ranging between 20 and 200 nM/cm<sup>2</sup> yr. Sediment slurry incubations conducted to determine the mechanisms and rate of arsenic biogeochemical transformations in these sediments confirm that any arsenate added to these sediments is immediately adsorbed and later released during the reductive dissolution of iron oxides. Incubations in the presence of low concentrations of arsenate verified that microbial iron reduction occurs in these sediments and that arsenate is not concomitantly reduced during this process. Incubations with higher initial arsenate concentrations indicate that the microbial processes in these sediments may be affected by high inputs of arsenic. Finally, differences between high discharge rates and base-flow conditions in the Chattahoochee River do not seem to affect the biogeochemical processes involved in iron and arsenic cycling but may enhance fluxes across the sediment-water interface.

This investigation was part of the Ph.-D. dissertation of Stephanie Chow and has contributed to the training of several other undergraduate (Jimmy Elsenbeck, Jennifer King, Dian Putrasahan, Farhana Yasmin) and graduate (Gwendolyn Bristow, Elizabeth Carey, Judson Partin) students working under Dr. Taillefert's direction. These students either participated in field trips or performed some of the reported chemical analyses. This project resulted in the publication of one peer-reviewed paper (35), two presentations at professional meetings (American Chemical Society), one presentation at a local symposium (Georgia Tech), and one seminar (Savannah River Ecology Laboratory, UGA). Other abstracts and publications will follow in 2005.

## 2.0 Introduction

The adverse human health effects of arsenic have been known for several centuries. The toxicity and biochemical behavior of arsenic depends on its chemical form. In natural environments, arsenite ( $\text{H}_3\text{AsO}_3$ ) is not only more mobile but can be greater than 60 times more toxic than arsenate ( $\Sigma\text{AsO}_4^{3-}$ ), or organoarsenic compounds (1, 2). Reported regions impacted by elevated arsenic concentrations are Bangladesh, China, India, England, Thailand, and within the United States (e.g., New Hampshire, New Mexico, Massachusetts, Maine, Michigan, California, and Oregon). Arsenic input in the natural environment is mainly due to natural sources and coal-fire power plants because of its ubiquitous presence in coal (3). Coal-fire power plants release arsenic and other metalloids in the atmosphere during burning. However, the ashes are usually stored in ponds that may be episodically flooded during storm events and represent significant sources of arsenic for aquatic systems, especially nearby rivers which are often used for cooling purpose. Once in rivers, arsenic may be removed by adsorption onto sediments or travel downstream in solution (3).

In high concentrations, the most toxic fraction, arsenite, may affect ecosystems and can also present a risk for human health as these waters will eventually recharge water tables and/or lakes used for the supply of drinking water. The problem of arsenic is a main concern of the Georgia Environmental Protection Division of the Department of Natural Resources (<http://www.ganet.org/dnr/environ/>) and largely recognized in major cities, as part of the heavy metal class. However, it is equally important to evaluate locations where arsenic exists at low concentration due to its potential impact on drinking water resources.

Most environmental arsenic problems are a result of mobilization and reduction of arsenic regulated by biogeochemical processes at redox interfaces (4). In oxic conditions, authigenic iron, manganese, and aluminium oxides, clays, and particulate organic matter (POM) can remove metals by sorption or precipitation (5). The adsorption of arsenic in natural waters is mainly controlled by solid-solution interactions with iron oxides (1, 6-8) because their charge, in contrast to POM and manganese and aluminum oxides, is slightly positive at circumneutral pH (9), while arsenate is negatively charged (7, 10-12). As a result, arsenate mobility and bioavailability is limited in oxic conditions. In suboxic conditions, manganese and iron oxides are reductively dissolved during organic matter remineralization, potentially releasing trace metals including arsenate (4), in the dissolved phase. It is also suggested that arsenate may be simultaneously reduced during the reduction of iron oxides (13), thus turning arsenic-contaminated sediments into a persistent toxic source. However, little evidence of the simultaneous reduction of iron and arsenate has been found in natural systems.

In anoxic conditions, arsenate may be reduced to arsenite microbially (14-16) or chemically by dissolved sulfide (17) and  $\text{Fe}^{2+}$  (18, 19) though both chemical reactions are usually slow. Arsenite is neutral at circumneutral pH and is less susceptible to adsorption onto metal oxides (7, 10, 11). In the presence of dissolved sulfide produced by sulfate-reducing bacteria, arsenite may form thioarsenite complexes (20) and eventually precipitate as arsenosulfide minerals (21, 22) or, alternatively, adsorb onto iron sulfide minerals (22). These thioarsenite complexes have yet to be identified in natural waters but, if they exist, the solubility of arsenite may be enhanced in the presence of  $\text{H}_2\text{S}$ , providing a source of toxic compound in the natural environment.

Finally, arsenite can be rapidly reoxidized in the presence of dissolved oxygen (23) or

manganese oxides (24, 25). Thus, desorption and remobilization of arsenic from sediments is influenced by pH, the activity of microorganisms, and the concentrations of dissolved oxygen, sulfide and iron in interstitial waters (8, 10, 22, 28-31). In addition, phosphate, bicarbonate, silicate and organic matter all compete with arsenic for adsorption sites, enhancing arsenic desorption and thus mobility (31).

### 3.0 Objectives

It is clear that arsenic is subject to several complex transformations in aquatic systems. As the sediment is usually the ultimate repository of trace metals and metalloids, it is necessary to determine quantitatively the fate of arsenic in these systems. In this project, we proposed to investigate the cycling of arsenic in the sediment of the Chattahoochee River to determine if and by what mechanism arsenic is accumulated in the sediment downstream from two coal-fire power plants and how arsenic is biogeochemically transformed in these sediments. The specific questions we proposed to answer in this project were the following:

**1/ Does arsenic accumulate in the sediment, is remobilized, and diffuse back into the water column episodically after storm events?**

**2/ What are the main biogeochemical process regulating the transformation of arsenic in these iron-rich riverine sediments?**

To answer question 1, we proposed to monitor in situ the depth profiles of dissolved oxygen, Mn(II), Fe(II), and  $\Sigma\text{H}_2\text{S}$  at one site in the sediment of the Chattahoochee River downstream from the suspected arsenic source before, during, and after a storm. Unfortunately, deployment of our in situ instrument presented logistical problems. We could not find a boat that could deploy our heavy instrumentation on the Chattahoochee River. We therefore decided to collect sediment cores and use a non-invasive ex situ approach to monitor depth profiles of the main redox species involved in arsenic cycling at different sites along the river. After completion of the ex situ measurements, sediment porewaters were extracted, and the concentration of dissolved arsenic ( $\text{As}_d$ ) and arsenite as well as the major ions involved in the cycling of arsenic were determined. Finally, solid phase extractions were performed to quantify amorphous iron oxides and total extractable arsenic ( $\text{As}_t$ ).

To answer question 2, sediments were collected at the monitoring points according to their chemical characteristics and sediment slurries manipulated in batch reactor experiments. The slurries were analyzed as a function of time for arsenite,  $\text{As}_d$ , Fe(II), Mn(II), and  $\Sigma\text{H}_2\text{S}$ . Manipulations consisted in providing arsenate to the sediment slurries and following the evolution of the reactants and products over time to determine the reaction kinetics.

## 4.0 Sampling Site

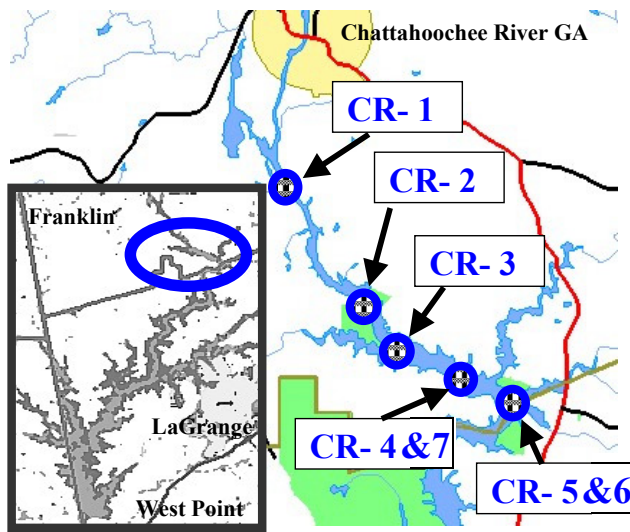


**Figure 1. Study Location in the Chattahoochee River upstream from West Point Lake (GA). Seven sediment cores, numbered CR-1 to -7, were collected along the Chattahoochee River during this study. Their locations are provided on the map.**

We selected our field site in the Chattahoochee River near West Point Lake, downstream from a point-source of arsenic in the water column (3). West Point Reservoir (inset Figure 1) is a 25,900-acre mainstream Chattahoochee River impoundment located an hour southwest of Atlanta (GA). West Point Lake lies on a 35 mile stretch of the Chattahoochee River between Franklin and West Point (GA). The lake has a shoreline of more than 500 miles and runs along and across the Georgia/Alabama State line. The lake is controlled by the Army Corps of Engineers and was impounded in 1974 to provide drinking water, flood control, hydroelectric power, navigation, wildlife development, and general recreation for Southwest Georgia.

**TABLE 1. Water Levels (feet) and Discharge (cfs) Measured in the Chattahoochee River at West Point, GA (USGS Station #02339500) Around the Time of Sampling During Three Consecutive Years (2002, 2003, 2004).**

Date	Time	Water Level	Discharge
		[feet]	[cfs]
6/11/2002	7:10	2.28	647
6/25/2002	8:15	2.24	816
9/5/2002	8:25	2.1	748
5/9/2003	10:54	21.42	65500
5/9/2003	19:26	20.64	63600
5/10/2003	11:05	19.75	60300
5/12/2003	13:25	8.88	16990
8/6/2003	10:45	5.16	6850
4/5/2004	8:50	6.16	9210
12/1/2004	14:33	5.84	7995

Seven sediment cores (Figure 1) were collected from the outfall of the Chattahoochee River north of the drinking water reservoir of West Point Lake in LaGrange (GA) based on elevated total dissolved arsenic concentrations detected in the water column (3). Our study focused in an area approximately 60 km away from the suspected arsenic source where total dissolved arsenic was depleted from the water column. The sediment cores were collected in July 2003, three weeks

after Tropical Storm Bill brought approximately 20 foot crests through the study location, and in May 2004, when the Chattahoochee River was at base-flow conditions (Table 1).

## 5.0 Methods

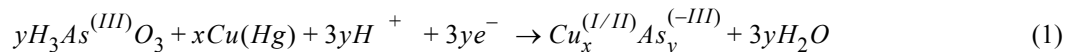
Sediment samples were collected with 60 cm long and 10 cm diameter polycarbonate core liners. Approximately 10 cm of overlying water was collected with each core to maintain the integrity of the sediment-water interface and minimize exposure to the atmosphere during transport to the laboratory. To answer question 1, we determined depth profiles of redox geochemical species at a millimeter resolution in selected sediment cores with gold-mercury (Au/Hg) voltammetric microelectrodes (32). Voltammetric techniques are attractive to measure chemical species in sediments because they can detect several analytes at once, they have low detection limits, and generally do not suffer from matrix problems (e.g., high salinity). Voltammetric microelectrodes have been successfully built and are routinely utilized in our group for field deployments (33, 35) or laboratory investigations (34). High resolution voltammetric and potentiometric profiles of  $O_{2(aq)}$ ,  $Fe^{2+}$ ,  $Mn^{2+}$ ,  $\Sigma H_2S$  ( $H_2S$ ,  $HS^-$ ,  $S^0$ ,  $S_x^{2-}$ ), organic- $Fe^{(III)}_{(aq)}$ ,  $FeS_{(aq)}$ , and pH were obtained by lowering an Au/Hg voltammetric microelectrode and a pH minielectrode (Diamond General Corp.), in millimeter increments, into each sediment core with a micro-manipulator (Analytical Instrument Systems, Inc.).

Voltammetric and pH measurements were conducted with a DLK-100A potentiostat that includes a voltmeter for combination measurements (Analytical Instrument Systems, Inc.). Dissolved oxygen was measured cathodically by linear sweep voltammetry, while  $Fe^{2+}$ ,  $Mn^{2+}$ , organic- $Fe^{(III)}_{(aq)}$ ,  $\Sigma H_2S$ , and  $FeS_{(aq)}$  were detected by cathodic square wave voltammetry. Prior to each scan, a conditioning step was applied at -0.1 V for 10 s to clean the microelectrode. Scan rates of 200 mV/s were used for all measurements (32). The pH was calculated using the Nernst Law after recording the potential and sample temperature at the minielectrode (36). By using microelectrodes, a suite of constituents could be measured with a high spatial resolution without sediment handling, thus minimizing contamination while maximizing the volume of porewater for other analyses.

Immediately following completion of the electrochemical profiles, the sediments were sectioned and centrifuged under  $N_{2(g)}$  atmosphere, and porewaters were filtered (Norm-Ject sterile Teflon syringe and Puradisc 0.2 $\mu$ m Whatman filter) and acidified with Trace Metal Grade HCl or  $HNO_3$  (Fisher) as needed for preservations and analysis. All porewaters were extracted and maintained in a  $N_{2(g)}$  atmosphere and kept at 4°C until analysis of As(III), total dissolved arsenic ( $As_d$ ), chloride, nitrate, sulfate, total dissolved orthophosphate, and total dissolved silica within 24 hours.

All solutions were prepared with 18 MW-cm Reverse Osmosis (RO) water (Barnstead). All plasticware and glassware used for trace metal analyses were acid-washed in 2% Trace Metal Grade  $HNO_3$  (Fisher) for one week and rinsed thoroughly with RO water. For As(III) analysis, standards were made from an As(III) stock solution prepared daily by dissolving As(III) oxide (Alfa Aesar) in NaOH then acidifying with 12 N HCl (37). Voltammetric measurements for As(III) were performed with a HMDE using the VA 663 multi-mode mercury drop electrode stand (Metrohm) coupled to the PGSTAT 12 Autolab potentiostat (Ecochemie). The reference electrode was an Ag/AgCl/KCl (3 M) with a 0.2 M NaCl glass bridge, and a glassy carbon rod acted as the

counter electrode. The solutions were thoroughly degassed with ultra high purity  $N_{2(g)}$  in between each As(III) measurement to prevent reoxidation by dissolved oxygen. As(III) concentrations were determined by amending the sample with 0.7 mM Cu(II) ( $CuCl_2 \cdot 2H_2O$  Aldrich) and 1 M HCl. A potential was applied at -0.4 V for 10 seconds to form an arseno-copper complex (Eq. 1 - deposition step) (37).



The potential was then scanned cathodically (from -0.4 V to -1.2 V) at 300 Hz using square wave voltammetry to reduce  $Cu^{(I/II)}$  from the arseno-complex to  $Cu^0$  and allow the indirect measurement of As(III) (Eq. 2 - stripping step).

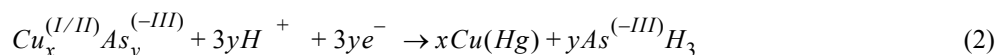
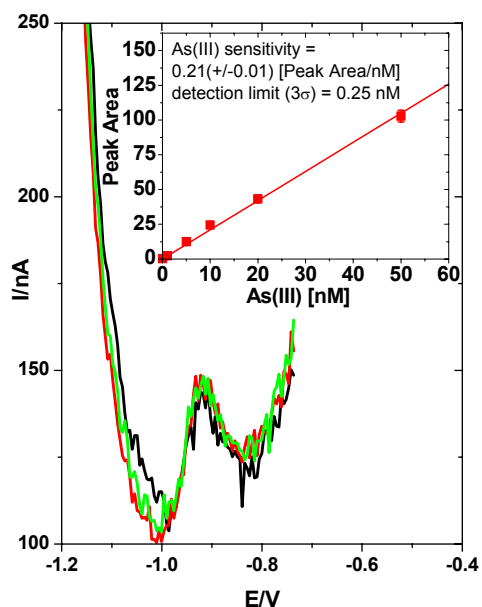


Figure 2 shows a triplicate raw data scan of a 1 nM As(III) standard. The detection limit of the method was 0.25 nM As(III) (at  $3\sigma$  of the blank).

Total dissolved arsenic concentrations ( $As_d$ ) were determined in triplicate with an Agilent - 7500a ICP-MS. Standards were prepared from a 1,000 ppm in 5%  $HNO_3$  As stock solution (Aldrich). An internal standard of 1 ppb germanium, prepared from 1,000 ppm stock solution (Aldrich) was added to standards and samples to correct for internal drift of the instrument. For quality control,  $As_d$  standards were inserted every 10 samples. The detection limit of  $As_d$  was found to be 0.25 nM.

Total dissolved phosphate and silica were determined by spectrophotometry (38, 39). Sulfate, nitrate, and chloride were measured by Ion Chromatography (Dionex Model 300X) with a bicarbonate buffer as eluent. Amorphous iron oxides were extracted in triplicate in selected samples using ascorbate reagent (40). Fe(II) produced during the extraction was analyzed with the Ferrozine Method (41). Total extractable arsenic ( $As_t$ ) was obtained from aqua regia digestions for 8h at 80°C (42).

Sediment slurry incubations with sediments from the CR-4 and CR-5 cores were used to determine the mechanisms of accumulation of dissolved arsenic and iron in the porewaters. These sediments were incubated in overlying water from the sites. A first set of incubations was conducted with sediments from three different depths in CR-4 and CR-5 to reflect the microbial community changes that may occur with depth in sediments. This first set of incubations was amended with a low constant concentration of 100 nM arsenate to reflect the porewater composition at these sites. A second set of incubations was conducted with the first 10 cm of sediments from CR-4 and CR-5 but with three different initial concentrations of arsenate to mimic a pollution event. All incubations were performed in sealed 25 ml Dellco



**Figure 2. Reproducibility of triplicate HMDE voltammetric measurements of a 1 nM As(III) standard. The inset shows a typical calibration curve. The method has a detection limit of 0.25 nM at three standard deviations from the blank**

Hungate tubes to maintain anaerobic conditions. The tubes and rubber stoppers (septa) were acid washed, rinsed, dried, and autoclaved to avoid contaminations. The slurries consisted of 5 g of sediment in each tube, to which 17 ml of autoclaved overlying water from the Chattahoochee River was added. Each reactor was degassed for 30 minutes before being sealed permanently with rubber stoppers and aluminum caps. They were kept in the dark and at room temperature but gently and constantly rotated to homogenize the slurries. At regular time intervals, 2 ml of porewaters were sampled through the rubber septa with a sterile polypropylene syringe. All sample extractions were performed under a nitrogen atmosphere to avoid oxidation of reduced metabolites. Subsamples were immediately analyzed for As(III) by HMDE (see above) and Fe(II) with the Ferrozine method. The remaining sample was acidified with 0.1 N HNO<sub>3</sub> (Fisher) and analyzed at a later stage for total dissolved As by ICP-MS. Abiotic control slurries were added to ensure that no oxygen penetrated the Hungate tubes and that no microbes were present in the autoclaved overlying water from the Chattahoochee River.

## 6.0 Results

The sediment cores collected in July 2003 were both anoxic, with dissolved oxygen decreasing from approximately 280  $\mu\text{M}$  in the overlying water to undetectable levels just below the sediment-water interface (Figure 3a and Figure 4a). As illustrated on Figure 3b, the pH decreased from 6.4 just below the SWI to 6.1 at 20 mm, then stabilized until 50 mm where it decreased again to reach 5.8 at 80 mm. Fe(II) rose from undetectable levels ( $< 5 \mu\text{M}$ ) within 10 mm from the SWI to a maximum of 940  $\mu\text{M}$  in CR-4 (Figure 3a) and 540  $\mu\text{M}$  in CR-5 (Figure 4a). It then stabilized around these values until 40 mm in both CR-4 and CR-5. While Fe(II) abruptly increased in CR-5 to a maximum of 550  $\mu\text{M}$  before decreasing regularly to a minimum of 100  $\mu\text{M}$  at 80 mm, it oscillated between 500 and 900  $\mu\text{M}$  below 40 mm in CR-4. Mn(II) concentrations displayed similar behaviors in both CR-4 and CR-5, except that Mn(II) was produced at 5 mm below the SWI in CR-4 and directly at the interface for CR-5. It increased to reach a maximum of 590  $\mu\text{M}$  between 45 and 55 mm in CR-4 (Figure 3a) and 470  $\mu\text{M}$  between 20 and 30 mm in CR-5 (Figure 4a). Below these depths, Mn(II) decreased in both cores to approximately 100  $\mu\text{M}$ . No  $\Sigma\text{H}_2\text{S}$  (detection limit  $< 0.2 \mu\text{M}$ ) were detected in these sediments. Chloride concentrations were approximately 130  $\mu\text{M}$  in the first 10 cm of the sediment then slightly decreased to 100  $\mu\text{M}$ . Nitrate (Figure 3c) was detected in the overlying water only, at a concentration of 27  $\mu\text{M}$ . Sulfate concentrations were highest at 47  $\mu\text{M}$  in the overlying water then diminished regularly to below the detection limit of 2  $\mu\text{M}$  at 43 mm in CR-4 (Figure 3c).

Total dissolved phosphate and total dissolved silica (data not shown) were below detection limit in both cores. As(III) was not detected in the extracted porewaters using HMDE, even after increasing the deposition time from 60 to 600 s to improve the detection limit. We therefore conclude that total dissolved arsenic ( $\text{As}_d$ ) profiles (Figure 3d and Figure 4b) are indicative of arsenate only. In both cores, the concentration of As(V) was significant at the sediment-water interface, 25 nM in CR-4 and 75 nM in CR-5, and increased deeper to a maximum of 156 nM between 15 and 25 mm in CR-4 and 107 nM between 55 and 68 mm in CR-5. As(V) then decreased to a minimum of 15 nM between 125 and 135 mm in CR-4 and 20 nM between 95 and 105 mm in CR-5.

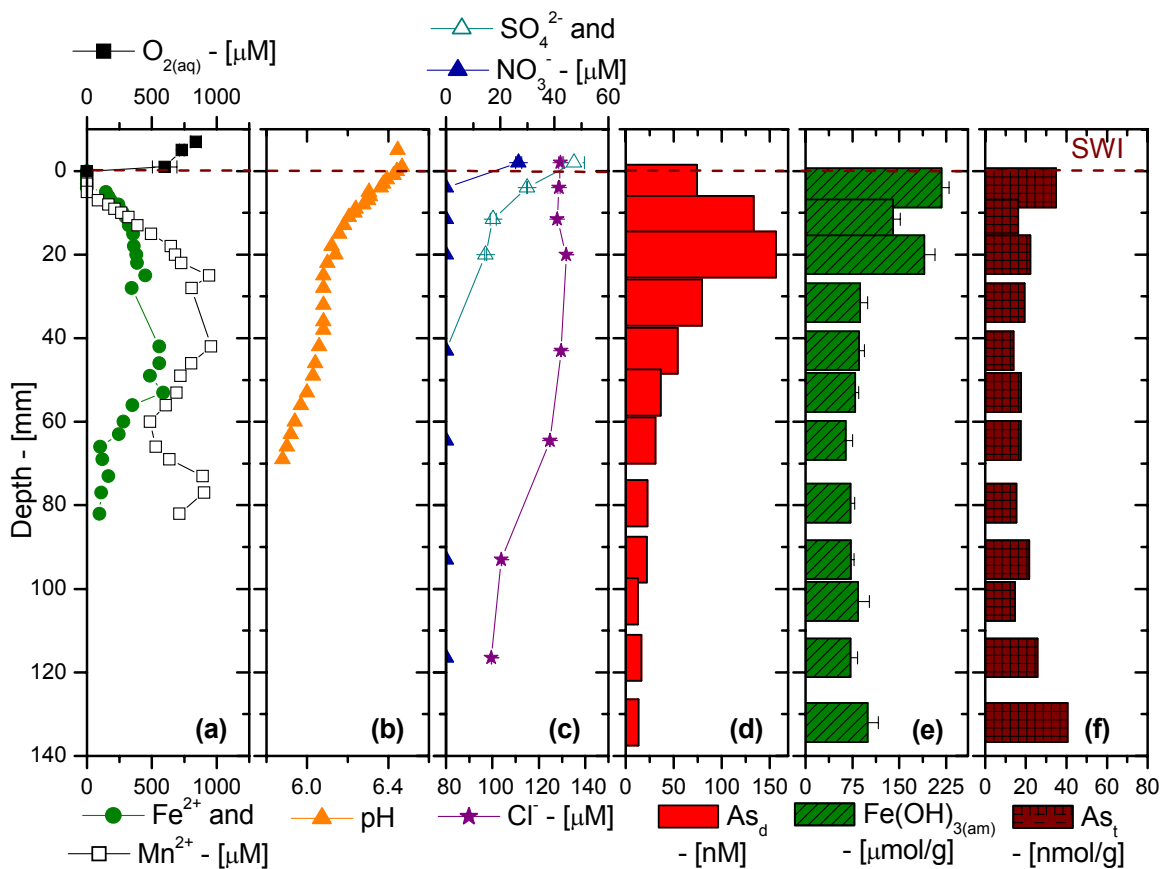


**Figure 3. Depth Profiles of: dissolved oxygen, Fe(II), and Mn(II) (a); pH (b); sulfate, nitrate and chloride (c); total dissolved arsenic (d); amorphous iron oxides (e); and total extractable arsenic (f) in CR-4 collected in July 2003 in the Chattahoochee River.  $\Sigma\text{H}_2\text{S}$  was below detection limit.**

The concentration of amorphous iron oxides, as determined by the ascorbate extraction, decreased with depth in CR-4, from  $170 \pm 6 \mu\text{mol/g}$  in the top 5 mm to  $75 \pm 8 \mu\text{mol/g}$  below 20 mm (the depth depicting the highest dissolved As(V) in the porewaters - Figure 3d and e). CR-5 results displayed a more variable profile with concentrations of amorphous iron oxides ranging between  $108 \pm 25 \mu\text{mol/g}$  in the first 50 mm and  $78 \pm 30 \mu\text{mol/g}$  between 60 mm (depth depicting the highest As(V) concentration - Figure 4b) and 120 mm. The concentration of total extractable arsenic followed the trends displayed by iron oxides in both cores, with concentrations ranging between 20 and 40 nmol/g in both cores (Figure 3f and Figure 4d). These data suggest that arsenic is adsorbed onto iron oxides and released in solution when iron oxides are reductively dissolved.

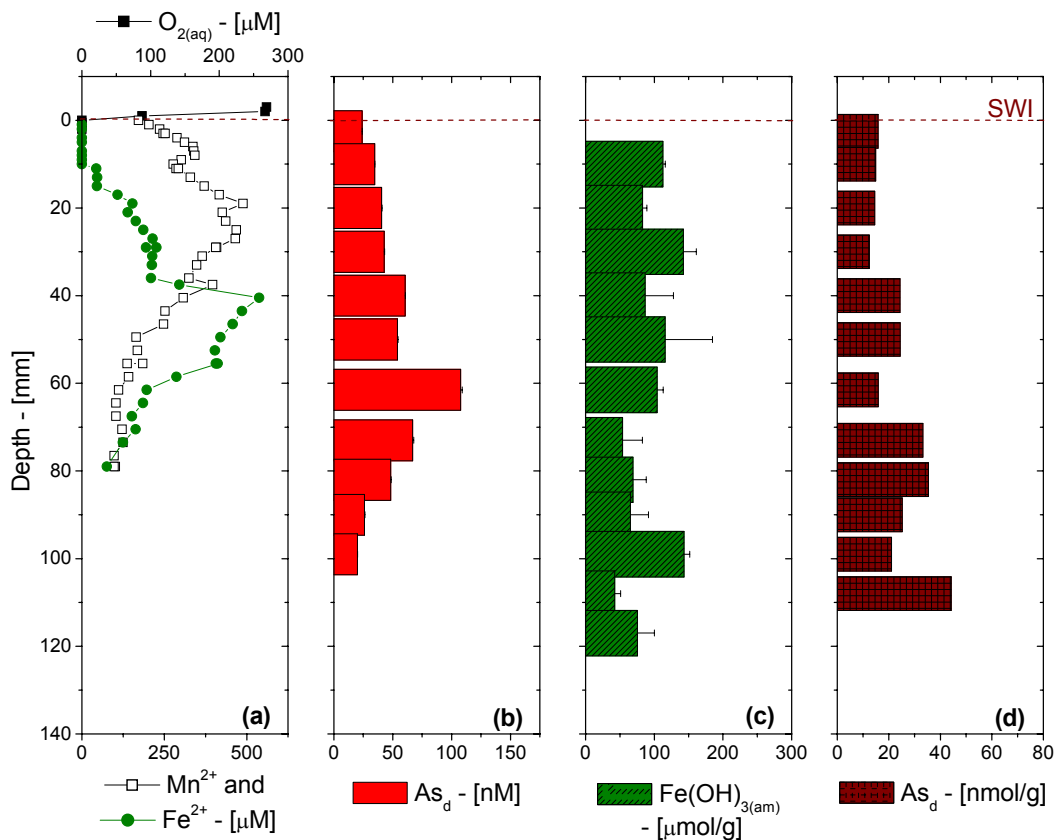


**Figure 4. Depth Profiles of: dissolved oxygen, Fe(II), and Mn(II) (a); total dissolved arsenic (b); amorphous iron oxides (c); and total extractable arsenic (d) in CR-5 collected in July 2003 in the Chattahoochee River.  $\Sigma\text{H}_2\text{S}$  was below detection limit.**

The sediment cores collected in May 2004 were, in a similar fashion, both anoxic, with dissolved oxygen decreasing from approximately 100-150  $\mu\text{M}$  in the overlying water to undetectable levels just below the sediment-water interface (Figure 5a and Figure 6a). In both cores, the pH decreased just below the sediment-water interface (Figure 5b and Figure 6b), indicating that respiration and denitrification were both ongoing in the first 10 mm of these sediments. Fe(II) was produced below the pH minimum in both cores and reached concentrations as high as 1 mM at about the same depth (30 mm) before decreasing to below detection limit at 70 mm in CR-6 (Figure 5a) and 500  $\mu\text{M}$  in CR-7 (Figure 6a). Mn(II) was detected in CR-6 but not in CR-7. Interestingly, both cores displayed new features not seen the previous year. First, soluble organic-Fe(III) was detected below the onset of Fe(II) in both cores (Figure 5b and Figure 6b). The voltammetric currents for these soluble complexes of Fe(III) were similar, with maximums around 100 nA. While soluble organic-Fe(III) was maintained at high levels in CR-7, it decreased to 50 nA below 50 mm in CR-6. Second, sulfur species were detected in both cores (Figure 5b and Figure 6c). In CR-6, a distinct voltammetric signal for  $\Sigma\text{H}_2\text{S}$  ( $= \text{H}_2\text{S} + \text{HS}^- + \text{S}^{2-} + \text{S}^{(0)} + \text{S}_x^{2-}$ ) was detected about 5 mm below the onset of Fe(II) and soluble organic-Fe(III), reached a maximum as high as 25  $\mu\text{M}$  at 25 mm, and stabilized deeper around 15  $\mu\text{M}$ . In CR-7,  $\text{FeS}_{(\text{aq})}$ , instead of  $\Sigma\text{H}_2\text{S}$ , was detected at the onset of Fe(II) and soluble organic-Fe(III) and reached a steady value around 30 nA below 25 mm. These features suggest that sulfide may be involved in arsenic cycling.

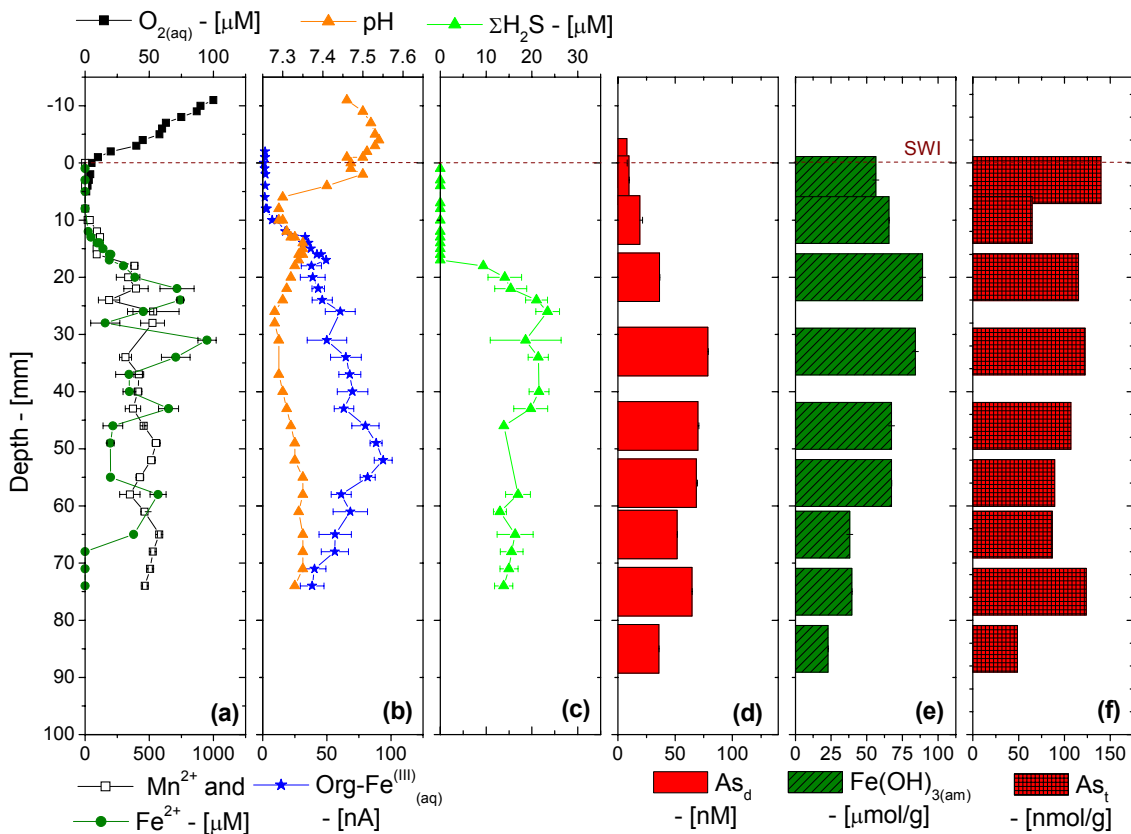


**Figure 5. Depth Profiles of: dissolved oxygen, Fe(II), and Mn(II) (a); pH and Org-Fe<sup>(III)</sup><sub>(aq)</sub> (b); ΣH<sub>2</sub>S (c); total dissolved arsenic (d); amorphous iron oxides (e); and total extractable arsenic (f) in CR-6 collected in May 2004 in the Chattahoochee River.**

Total dissolved arsenic ( $As_d$ ) in both cores fell in the range of concentrations detected the previous year (compare Figure 3d, Figure 4b, Figure 5d, and Figure 6c), and, likewise, arsenite was never detected. Therefore, dissolved arsenic was probably under the form of arsenate in these porewaters. In general, the dissolved arsenic depth profiles of both cores displayed similar trends.  $As_d$  increased below the sediment-water interface in both cores and reached a maximum of 75 nM at 35 mm in CR-6 (Figure 5d) and 115 nM at 65 mm in CR-7 (Figure 6c). Both profiles coincided with the onset of Fe(II) in these porewaters, suggesting that arsenate was released during the reductive dissolution of iron oxides.

Amorphous iron oxides behaved differently in both cores. CR-6 contained 50  $\mu\text{mol/g}$  iron oxides just below the sediment-water interface and displayed a maximum of 87  $\mu\text{mol/g}$  at 20 mm before decreasing regularly to 25  $\mu\text{mol/g}$  at 85 mm (Figure 5e). In contrast, amorphous iron oxides was more variable in CR-7, with concentrations as high as  $166 \pm 34 \mu\text{mol/g}$  (Figure 6d). Total extractable arsenic displayed the exact opposite. It was variable in CR-6, with concentrations ranging around  $100 \pm 30 \text{ nmol/g}$ , but CR-7 contained high background concentrations around  $200 \pm 30 \text{ nmol/g}$  at the surface and displayed a maximum of 550 nmol/g arsenic at 40 mm in the region where Fe(II) reached its maximum. Below 40 mm, it decreased back to the high background concentrations observed at the surface.

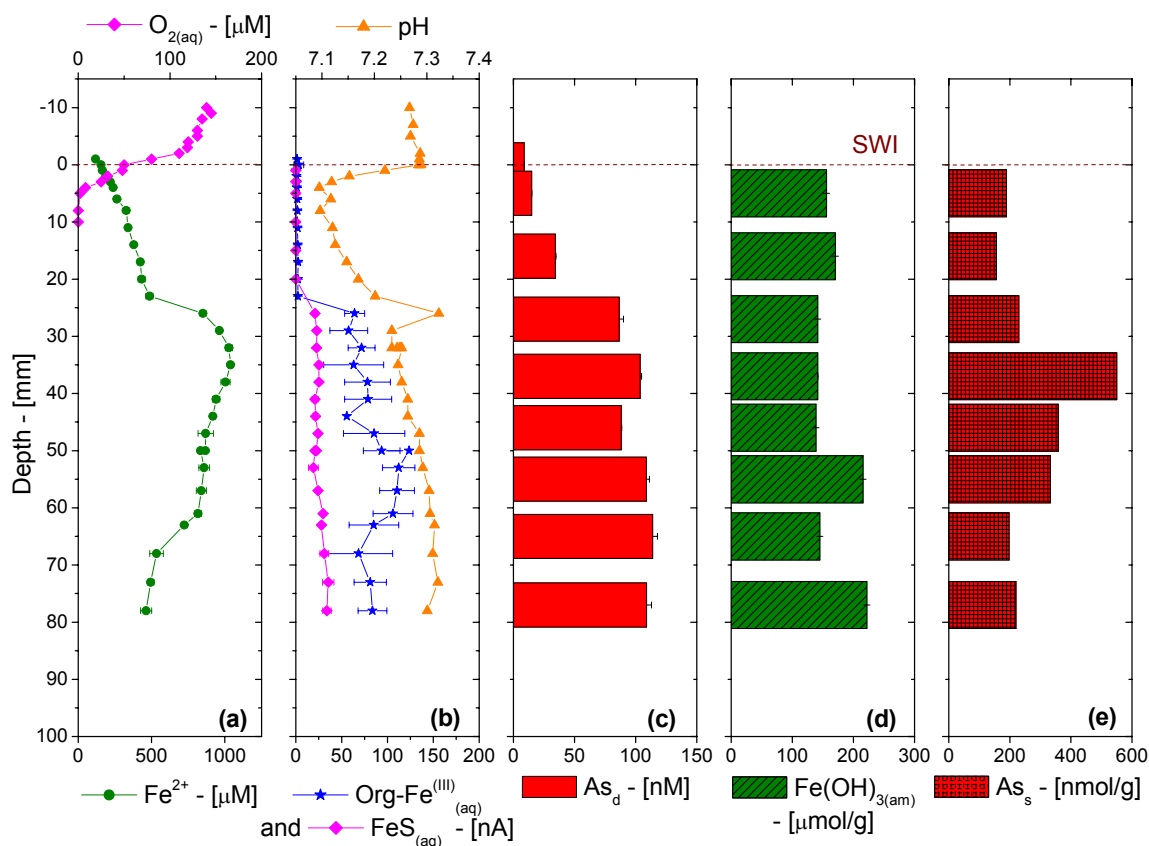


**Figure 6. Depth Profiles of: dissolved oxygen and Fe(II) (a); pH,  $Org-Fe^{(III)}_{(aq)}$ , and  $FeS_{(aq)}$  (b); total dissolved arsenic (c); amorphous iron oxides (d); and total extractable arsenic (e) in CR-7 collected in May 2004 in the Chattahoochee River.  $\Sigma H_2S$  and Mn(II) were below detection limit.**

The first set of incubations was conducted with sediments from CR-4 and CR-5 in the presence of a low concentration of arsenate (100 nM) to mimic the maximum concentration of dissolved arsenic measured in the porewaters (Figure 3d and Figure 4b). These incubations were conducted using sediments from the surface (0-15 mm in CR-4 and 5-25 mm in CR-5), intermediate depths (15-38 mm in CR-4 and 55-78 mm in CR-5), and deep depths (71-98 mm in CR-4 and 94-112 mm in CR-5) to reflect the fact that the microbial communities responsible for the transformation of iron and arsenic may be different at these locations. All the incubations showed that iron oxides were reduced and produced much higher Fe(II) concentrations than measured in the porewaters samples. Iron reduction rates were similar between the surface and the intermediate-depth sediments in both cores (Figure 7a, b, d, and e). In turn, incubations with the deepest sediments at both sites showed a phase lag of about 60 days before iron reduction took place. These data logically suggest that microbial communities were much more difficult to activate in the deeper sediments. Interestingly, about 50% of the arsenate initially added to the slurries was instantaneously removed from the porewaters, and only a fraction of the total amendment was recovered in the porewaters during these incubations. Speciation measurements in the dissolved phase of these samples revealed that arsenite was never produced during these incubations.

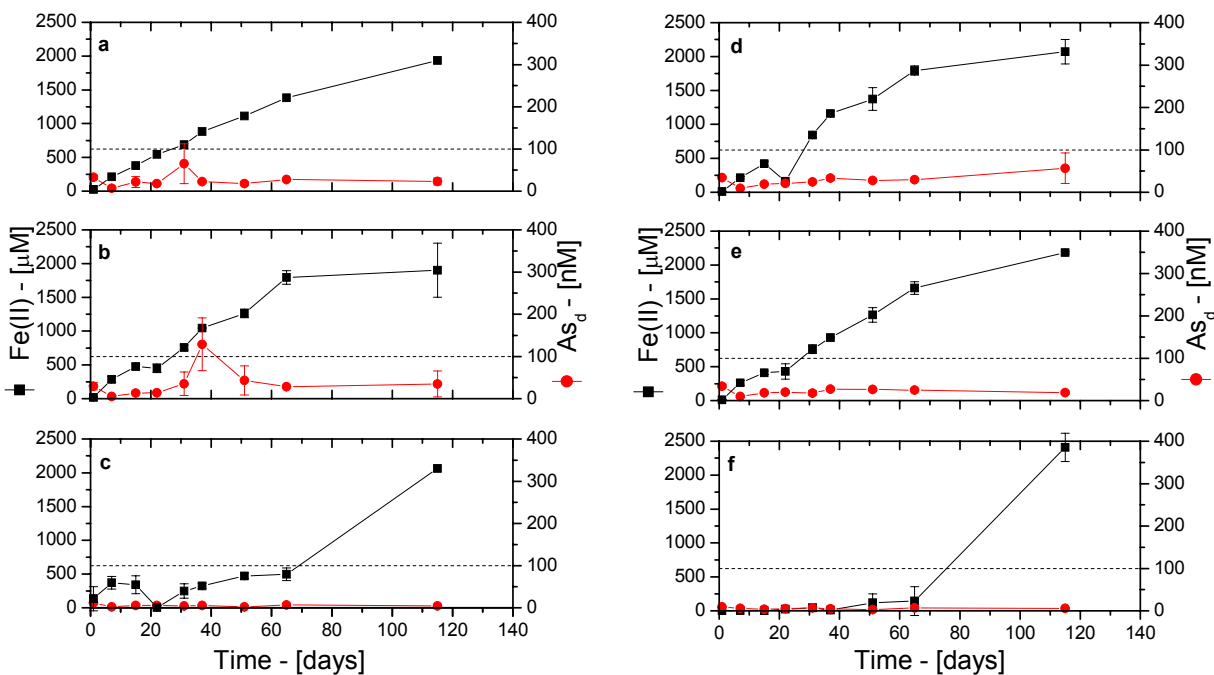


**Figure 7. Fe(II) and total dissolved arsenic (As<sub>d</sub>) produced during sediment slurry incubations amended with 100 nM arsenate in West Point Lake overlying water: surface sediment from CR-4 (a); CR-4 sediment from intermediate depths (b); deep sediment from CR-4 (c); surface sediment from CR-5 (d); CR-5 sediment from intermediate depths (e); and deep sediment from CR-5. The dash line represents the initial concentration of arsenate added to each slurry (right axis).**

A second set of incubations was conducted to simulate the effect of a contamination by arsenate. This time, the sediments from the surface and intermediate depths of CR-4 and CR-5 were respectively mixed into two large samples, and three treatments for each sediment were selected, with respective amendments of 0, 1, and 10 μM arsenate. These incubations are still ongoing but already show interesting results (Figure 8). First, the control slurries (no amendment) show significant release of dissolved arsenic into the porewaters (Figure 8a and d), with concentrations reaching that measured in the sediment cores (Figure 3d and Figure 4b). The accumulation of dissolved arsenic is accompanied by the accumulation of Fe(II), with concentrations in the same range as measured in the porewaters (Figure 3a and Figure 4) and during the first 30 days of the first set of incubations (Figure 7). These results suggest that these incubations are reproducible. It is also interesting to observe that the incubations performed with the 1 μM arsenate amendments (Figure 8b and e) very rapidly produce in both sediments higher concentrations of Fe(II) than the no amendment controls (Figure 8a and d). Simultaneously, dissolved arsenic, which was almost completely removed from the porewaters initially, is produced in much higher concentrations during the course of the incubations than in the no amendment controls. In turn, the highest arsenic amendment incubations in both CR-4 and CR-5 sediments (Figure 8c and f) release the same Fe(II) concentrations as in the no amendment controls (Figure 8a and d), while dissolved arsenic, initially completely removed from the porewaters, is slowly produced in higher concentrations than both the no amendment controls and the 1 μM amendment. These incubations show that only a fraction of the total arsenate added has been released in the porewaters. They will be pursued until 100% recovery is reached.

Preliminary speciation measurements indicate that As(III) can be detected in both the 1 and 10  $\mu\text{M}$  arsenic amendments after 30 days, suggesting that arsenate reduction must occur in these sediments.

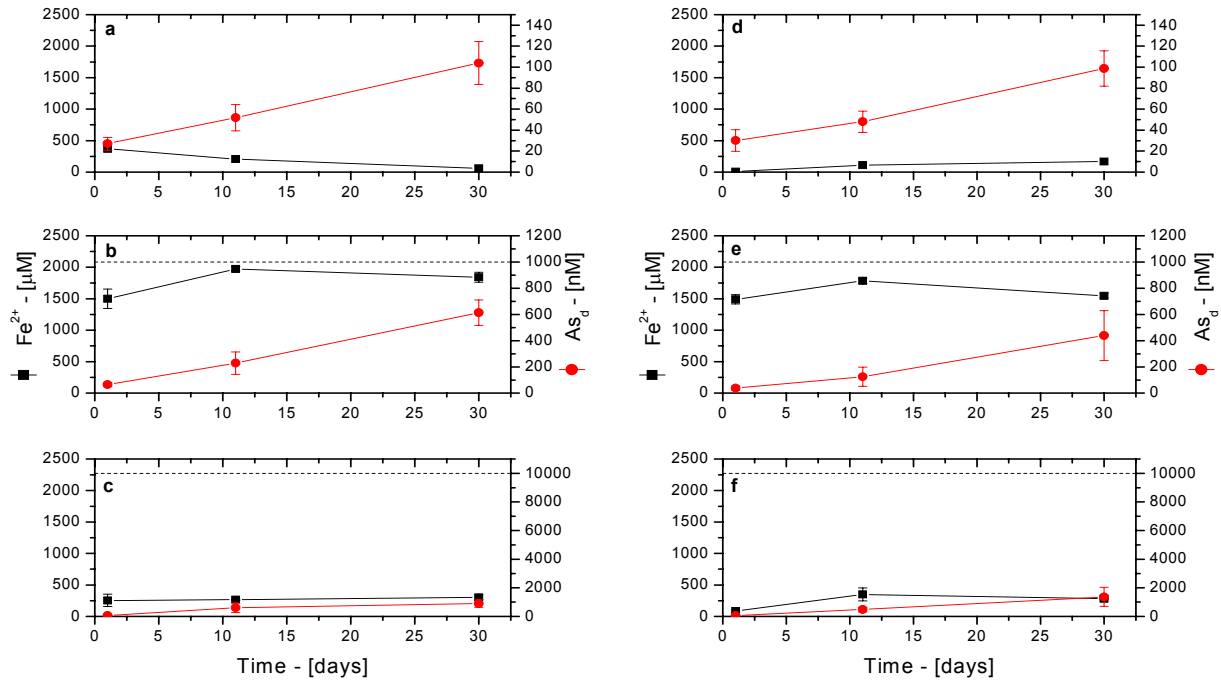
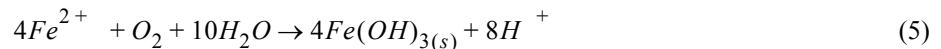
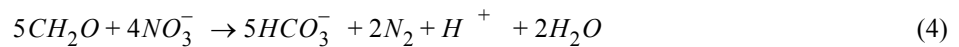


**Figure 8.** Fe(II) and total dissolved arsenic ( $\text{As}_d$ ) produced during sediment slurry incubations amended with different initial arsenate concentrations in West Point Lake overlying water: CR-4 sediment with no amendment (a); CR-4 sediment amended with 1  $\mu\text{M}$  As(V) (b); CR-4 sediment amended with 10  $\mu\text{M}$  As(V) (c); CR-5 sediment with no amendment (d); CR-5 sediment amended with 1  $\mu\text{M}$  As(V) (e); and CR-5 sediment amended with 10  $\mu\text{M}$  As(V). The dash line represents the initial concentration of arsenate added to each slurry (right axis).

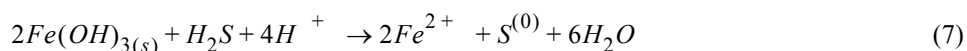
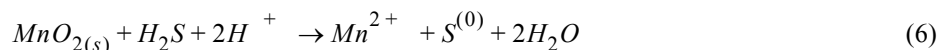
## 7.0 Discussion

Altogether, the chemical profiles provide a clear picture of the processes regulating the cycling of arsenic near the sediment-water interface. The rapid decrease in dissolved oxygen close to the SWI in each sediment core analyzed indicates that these sediments are anoxic. The generally low concentration of Fe(II), the absence of nitrate, and the decrease in pH near the SWI suggest that a combination of aerobic respiration (Eq. 3), denitrification (Eq. 4), and chemical oxidation of Fe(II) (Eq. 5) occur within the first centimeter of these sediments:

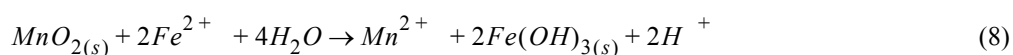


Iron oxidation is confirmed by the high concentration of amorphous iron oxides detected in the upper sediment of CR-4 and CR-6. Additionally, manganese and iron oxide reduction is demonstrated with the production of Mn(II) and Fe(II) within the first 3 to 4 cm of these sediments (Figure 3a to Figure 6a). The occurrence of metal reduction leads to a subsequent

stabilization of the pH in the sediment porewaters (Figure 3b, Figure 5b, and Figure 6b) because these reactions consume protons (36). Chemical reduction of manganese and iron oxides by dissolved sulfide (Eq. 6 and Eq. 7) may occur in sediments. However, the maximum concentration of dissolved sulfide available from the sulfate present in these freshwater sediments (i.e. 50  $\mu\text{M}$ ) is not high enough to account for all the Mn(II) and Fe(II) produced (compare maximum sulfate to maximum Mn(II) and Fe(II) concentrations in Figure 3 and Figure 4 for example).



Similarly, the chemical reduction of manganese oxides by Fe(II) is also possible (Eq. 8) but is usually slow above pH 4 (43).



It can therefore be concluded that most of the reduction of manganese and iron oxides is microbial in these sediments. Interestingly, Mn(II) reaches the sediment-water interface in core CR-5, suggesting that it diffuses out of the sediment at this location. This feature is well known and due to the slow oxidation kinetics of Mn(II) at circumneutral pH in the presence of oxygen (44). The disappearance of sulfate within the first 40 mm of CR-4 (Figure 3c) and the occurrence of  $\Sigma\text{H}_2\text{S}$  and  $\text{FeS}_{(\text{aq})}$  in CR-6 (Figure 5c) and CR-7 (Figure 6b), respectively, suggest that sulfate reduction proceeds in these sediments. In the sediments where dissolved sulfide was not detected in the porewaters, it must have been removed by precipitation as FeS. Interestingly, thermodynamic calculations with MINEQL+ using an average pH of 6.1, Fe(II) concentration of 800  $\mu\text{M}$  and assuming 50  $\mu\text{M}$   $\text{H}_2\text{S}$  (i.e. the maximum sulfate measured) produced in these sediments indicate that the solubility product of  $\text{FeS}_{\text{am}}$  and mackinewite are not exceeded. At this point, it is not clear if the system is not at equilibrium or if the thermodynamic database is inaccurate. Nevertheless, these profiles indicate that  $\text{H}_2\text{S}$  is produced episodically in these sediments and must have a significant impact on the cycling of arsenic.

Arsenic is thought to enter the Chattahoochee River upstream of the study location and is transported in the oxic river water in the form of As(V) (3). As As(V) flows downstream, it may adsorb onto colloidal and particulate matter contained in the river and settle to the sediment-water interface. The data indicate that this sediment is not a natural source of arsenic, since the concentration of dissolved arsenic in all sediment cores, except for CR-7 (Figure 6c), is higher near the SWI and depleted at depth. Therefore, these data support earlier hypothesis that the anthropogenic input of arsenic is significant in the Chattahoochee River (3).

The role of manganese and iron on the arsenic cycle has been investigated extensively (8, 10-12, 17-19, 22, 24-26, 30). In these sediments, adsorption of arsenic should dominate in the upper sediments which contain the highest concentration of amorphous iron oxides. The adsorption of arsenic is also affected by the degree of crystallization of the iron oxides because the density of adsorption sites decreases as the minerals are more crystallized (45). To determine the extent of adsorption of As(V) onto iron oxides in the first centimeters of these sediments, we implemented a double-layer surface adsorption model with MINEQL+ using parameters from the literature (45). The model assumes a specific surface area of 600  $\text{m}^2/\text{g}$  for amorphous iron oxides and two types of binding sites: high affinity sites with a density of 5  $\text{mmol}/\text{mol}$  Fe and low affinity sites

with a density of 0.2 mol/mol Fe. The input concentrations used in the model are based on the data of Figure 3 and Figure 4 (pH = 6.4;  $[\Sigma\text{AsO}_4^{3-}] = 150 \text{ nM}$ ;  $[\text{Cl}^-] = 130 \text{ }\mu\text{M}$ ;  $[\text{Fe}^{2+}] = 10 \text{ }\mu\text{M}$ ;  $[\text{SO}_4^{2-}] = 50 \text{ }\mu\text{M}$ ) or are estimated from previous work in the area (i.e. DIC = 300  $\mu\text{M}$ ). Assuming a sediment density varying between 0.98 and 0.87 g/cm<sup>3</sup> in clayey and silty sediments (46), the molar concentration of amorphous iron oxides is ca. 0.05 M. The model calculation predicts that 97% of the arsenate in our system is adsorbed onto iron oxides.

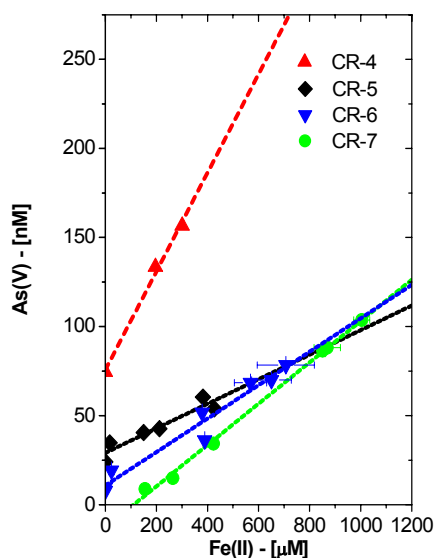
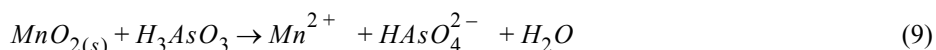


**Figure 9.** Correlation between Fe(II) and As(V) between 0 and 25 mm in CR-4, 40 mm in CR-5, 65 mm in CR-6, and 47 mm in CR-7.

As(V) is produced simultaneously with Fe(II) in the first few centimeters of each sediment investigated (Figure 3 to Figure 6). A positive correlation exists between Fe(II) and As(V) in all the cores, though with different slopes (Figure 9). From the slopes, a As:Fe(II) ratio of 3:10,000 in the top 25 mm of CR-4, 6:100,000 in the top 40 mm of CR-5, and 1:10,000 in the top 65 and 47 mm of, respectively, CR-6 and CR-7 were found. These data indicate that adsorbed arsenic may be released during the reduction of iron oxides, thus confirming the significant role of iron in the arsenic cycle. These data also indicate that more arsenate is scavenged onto iron oxides in CR-4 than any of the other cores. Silicates and phosphate were below the detection limit in all cores, suggesting they probably do not significantly effect arsenic mobilization in this system.

Mn(II) depth profiles indicate that the reduction of manganese oxides occurs in these sediments, however their involvement with arsenic is not evident. First, adsorption is not favored because at circumneutral pH, manganese oxides are negatively charged (9) while As(V) is mainly deprotonated (4). It is also known that manganese oxides oxidize arsenite to arsenate (25-27) according to:



However, there is an inconsistent correlation between Mn(II) and As(V) in all the cores (not shown). The lower adsorption affinity of As(V) onto manganese oxides at circumneutral pH along with the poor correlation between Mn(II) and As(V) suggest that manganese oxides play a minor role in the arsenic cycle in these sediments.

As previously mentioned, sulfate disappears in these porewaters suggesting that sulfate reduction may occur in these sediments. It has been shown recently that dissolved sulfide may slowly reduce As(V) and complex As(III) in the form of electrochemically inactive  $\text{AsO}_x\text{S}_y$  (20, 21) that could then undergo precipitation. Our measurements, however, could not detect any As(III) in solution in these sediments. We ruled out the possible oxidation of our samples after porewater extraction since the sediment cores were sectioned, centrifuged, filtered, acidified, and stored at 4°C under a  $\text{N}_{2(g)}$  atmosphere until As(III) analysis, which was conducted within 24 hours after collection. In addition, the arsenosulfide complexes, if present, should be dissociated in the acidic conditions of the As(III) analysis (pH 1) and detected electrochemically.

The fact that the sediment is reduced but arsenic is oxidized may be due to the dynamic nature of the system studied. The first two surficial sediments evaluated in this study (CR-4 and CR-5) were most likely deposited after the passage of Tropical Storm Bill, which impacted the site three weeks prior to this investigation. It is possible that the kinetically slow reduction of As(V) had not occurred so soon after deposition, while microbial iron reduction released As(V) in solution. Finally, the presence of As(V) and Fe(II) at deeper locations in CR-5 as compared to CR-4 is probably due to the more turbulent river flow at CR-5 which may bring dissolved oxygen to the sediment and increase erosion. This process is evidenced by a general decrease in both the Fe(II) and amorphous iron oxide concentrations in the sediment of CR-5 compared to CR-4 (Figure 3 and Figure 4). Interestingly, the last two sediment cores investigated in this study were obtained at base-flow conditions for the Chattahoochee River (Table 1). Yet our speciation measurements did not evidence any As(III), though conditions in these sediments were more reducing, with the occurrence of both dissolved sulfide (Figure 5c) and  $FeS_{(aq)}$  (Figure 6b), a precursor of  $FeS_{(s)}$  precipitation (36).

Diffusive fluxes were calculated for each core using Fick's Law with the molecular diffusion coefficient of phosphate as a proxy for that of arsenate ( $9.1 \times 10^{-5} \text{ cm}^2/\text{sec}$  for  $H_2PO_4^-$ ). According to these calculations, approximately 20 to 200 nM/cm<sup>2</sup>yr of arsenic may be diffusing into the overlying water column from the sediment depending on the flow conditions in the Chattahoochee River. Although the arsenic concentrations detected in the porewaters are not considered high compared to contaminated sites, the data suggest that arsenic is remobilized and may impact the drinking water reservoir located downstream.

The sediment incubations show that arsenate spiked to the sediment is initially very rapidly removed from the porewaters, most likely by adsorption onto iron oxides. These incubations also show that iron reduction occurs in these sediments and that dissolved arsenic is released concomitantly with the production of Fe(II). Our speciation measurements reveal that arsenic is under the form of arsenate only when the initial concentration of arsenic is in the range of that found in the porewaters, suggesting that arsenate reduction does not occur in the sediments of the Chattahoochee River. The second set of incubations show that when the initial concentration of arsenic injected to the sediment is elevated, some reduction may occur, though more data are needed at this point. In addition, it appears that microbial iron reduction is affected by elevated concentrations of total dissolved arsenic (Figure 8). Arsenic is a toxic compound that, in high concentration, may inhibit microbial processes.

The first set of incubations was used to calculate the rate of iron reduction assuming a first order with respect to iron oxides and zero order with respect to the reductant (Eq. 10). The reductant could either be dissolved sulfide, if its concentration is high enough, or natural organic matter if iron-reducing bacteria are involved in the transformation of iron oxides. From our field measurements, we can conclude that the involvement of dissolved sulfide in the production of Fe(II) is not significant. Therefore, these rates likely represent rates of microbial iron reduction in these sediments. The rate law of iron reduction is:

$$\frac{d}{dt}[Fe^{2+}] = k[Fe(OH)_{3(s)}] = k([Fe(OH)_{3(s)}]^0 - [Fe^{2+}]) \quad (10)$$

where k is the rate constant ( $d^{-1}$ ),  $[Fe(OH)_{3(s)}]^0$  is the initial concentration of iron oxides ( $\mu\text{M}$ ) in these sediments. This rate law has an analytical solution that was used to fit the rate constant k to

the data of Figure 7 using a least-square fitting procedure. The initial concentration of iron oxides was calculated from the sediment extraction measurements (Figure 3e and Figure 4c) assuming a sediment density of 0.78 g/cm<sup>3</sup> (46). Table 2 reports the rate constants determined for each incubation described in Figure 7, except for the deep depths, which displayed a phase lag, as there was not enough data to provide accurate rate constants. From these calculations, it is obvious that the rate of reduction increases with depth in these sediments. So far, the incubations cannot be used to provide rates of release of arsenate in the porewaters. These ongoing incubations will provide this information at a later time.

**TABLE 2. Sediment Depths Used in the First Set of Incubations (Figure 7), Initial Concentration of Amorphous Iron Oxides Measured in these Sediments and Used in the Model, and First Order Rate Constant (k) Determined in Each of these Incubations. ND = not determined.**

Core	Depth Incubated [mm]	[Fe(OH) <sub>3(s)</sub> ] <sup>0</sup> [μmol/g]	k [1/d]
CR-4	0-15	178.8	0.0198
CR-4	15-38	120.8	0.0203
CR-4	71-98	73.01	ND
CR-5	5-25	97.7	0.0164
CR-5	55-78	90.0	0.0251
CR-5	94-112	83.6	ND

## 8.0 Conclusions

This study successfully combined several analytical techniques to determine the profiles of major redox species and the speciation of As(III) and As(V) with a high spatial resolution (i.e., < 10 cm) from four sediment cores collected a year apart at two locations in the Chattahoochee River. Results provide evidence of the accumulation of dissolved arsenic close to the sediment-water interface at both locations and at both time periods. Depth profiles also display a substantial correlation between the diagenetic processes involving iron and arsenic in these sediments. They suggest that iron oxides scavenge arsenic in the form of arsenate in the water column and settle to the sediment-water interface where they are reduced by iron reducing bacteria. As a result of microbial iron reduction, As(V) is released and accumulates in the porewaters near the sediment-water interface, where it can diffuse back to the overlying waters. Interestingly, As(III) was never found in the porewaters, suggesting that the reduction of As(V) is a slow process that was not occurring in these sediments. Incubations with sediment slurries conducted in the presence of low concentrations of arsenate verified that microbial iron reduction occurs in these sediments and that arsenate is not concomitantly reduced during this process. Incubations of the same sediments but amended with higher initial arsenate concentrations indicate that the microbial processes in these sediments may be affected by high inputs of arsenic, including those necessary for remediation or natural attenuation. Finally, differences between high discharge rates and base-flow conditions in the Chattahoochee River do not seem to affect the biogeochemical processes involved in iron and arsenic cycling but may enhance fluxes across the sediment-water interface.

## 9.0 References

1. Ferguson, F.; Gavis, J. *Wat. Res.* 1972, 6, 1259-1274.
2. Ryu, J.; Gao, S.; Dahlgren, R.A.; Zierenberg, R.A. *Geochim. Cosmochim. Acta* 2002, 66, 2981-2994.
3. Lesley, M.P.; Froelich, P.N. Proceedings of 2003 Georgia Water Resources Conference.
4. Smedley, P.L.; Kinniburgh, D.G. *Appl. Geochem.* 2002, 17, 517-568
5. Buffle, J. *Complexation Reactions in Aquatic Systems an Analytical Approach*; Halsted Press: a division of Wiley: New York, NY, 1988; p 692.
6. Cullen, W.; Reimer, K.J. *Chem. Rev.* 1989, 89, 713-764.
7. Jain, A.; Raven, K.P.; Loeppert, R.H. *Environ. Sci. Technol.* 1999, 33, 1179-1184.
8. Kneebone, P.E.; O'Day, P.A.; Jones, N.; Hering, J.G. *Environ. Sci. Technol.* 2002, 36, 381-186.
9. Stumm, W. *Chemistry of the Solid-Water Interface*; John Wiley and Sons, Inc.; New York, 1992.
10. Pierce, M.L.; Moore, C.B. *Wat. Res.* 1982, 16, 1247-1253.
11. Belzile, N.; Tessier, A. *Geochim. Cosmochim. Acta* 1990, 54, 103-1039.
12. Mucci, A.; Boudreau, B.; Guignard, C. *Appl. Geochem.* 2003, 18, 1011-1026.
13. Guo, T.; DeLaune, R.D.; Patrick Jr., W.H. *Environ. Intern.* 1997, 23, 305-316.
14. Ahmann, D.; Krumholz, L.R.; Hemond, H.F.; Lovley, D.R.; Morel, F.M.M. *Environ. Sci. Technol.* 1997, 31, 2923-2930.
15. Harrington, J.M.; Fendorf, S.E.; Rosenzweig, R.F. *Environ. Sci. Technol.* 1998, 32, 2425-2430.
16. Oremland, R.S.; Dowdle, P.R.; Hoefft, S.; Sharp, J.O.; Schaffer, J.K.; Miller, L.G; Blum, J.S; Smith, R.L; Bloom, N.S; Wallschlaeger, D. *Geochim. Cosmochim. Acta* 2000, 64, 3073-3084.
17. Rochette, E.A.; Bostick, B.C.; Li, G.C.; Fendorf, S. *Environ. Sci. Technol.* 2000, 34, 4714-4720.
18. Appelo, C.A.J.; Van Der Weiden, M.J.J.; Tournassat, C.; Charlet, L. *Environ. Sci. Technol.* 2002, 36, 3096-3103.
19. Charlet, L.; Bosbach, D.; Peretyashko, T. *Chem. Geol.* 2002,190, 303-319.
20. Wilkin, R.T.; Wallschlaeger, D.; Ford, R.G. *Geochem. Trans.* 2003,4, 1-7.
21. Sadiq, M. *Mar. Chem.* 1997, 31, 285-297.
22. Bostick, B.C.; Fendorf, S. *Geochim. Cosmochim. Acta* 2003, 67, 909-921.
23. Johnson, D.L.; Pilson, M.E.Q. *Environ. Lett.* 1975, 8, 157-171.
24. Scott, M.J.; Morgan, J.J. *Environ. Sci. Technol.* 1995, 29, 1898-1905.
25. Manning, B.A.; Fendorf, S.E.; Goldberg S. *Environ. Sci. Technol.* 1998, 32, 2383-2388.
26. Chiu, V.Q.; Hering, J.G. *Environ. Sci. Technol.* 2000, 34, 2029-2034.

27. Driehaus, W.; Seith, R.; Jekel, M. *Wat. Res.* 1995, 29, 297-305.
28. Andreae, M.O. *Limnol. Oceanogr.* 1979, 24, 440-452.
29. Xu, H.; Allard, B.; Grimvall, A. *Water Air Soil Pollut.* 1988, 57, 269-278.
30. Mok, W. A.; Wai, C.M. *Environ. Sci. Technol.* 1990, 24, 102-108.
31. Meng, X.K.; Guo, P.; Bang, S.; Bang, K.W. *Toxicol. Letters* 2002, 133, 103-111.
32. Brendel, P. J.; Luther, G. W.; III. *Environ. Sci. Technol.* 1995, 29(3), 751-761.
33. Bull, D. C.; Taillefert, M. *Geochem. Trans.* 2001, 13, 1-8.
34. Carey, B.; Taillefert, M. *Limnol. Oceanogr.* 2005, In Press.
35. Chow, S. S.; Taillefert, M. 2005. In: *Advances in arsenic research: Integration of experimental and observational studies and implications for mitigation* (O'Day, P. V., D.; Meng, X.; Benning, L. G., Eds.), ACS Symposium Series, Vol. 915, In Press.
36. Taillefert, M.; Rozan, T. F.; Glazer, B.T.; Herszage, J.; Trouwborst, R. E.; Luther III, G. W. 2001. In: *Environmental Electrochemistry: Analyses of Trace Element Biogeochemistry* (M. Taillefert; T. F. Rozan, Eds.). ACS Symposium Series, Vol. 811, Washington, D.C. 247-264.
37. Li, H.; Smart, R. B. *Anal. Chim. Acta* 1996, 325, 25-32.
38. Murphy J.R.; Riley J.P. *Anal. Chim. Acta* 1962, 27, 31-36.
39. Strickland, J.D.H. *J. Amer. Chem. Soc.* 1952, 74, 862-876.
40. Kostka, J.E.; Luther III, G.W. *Geochim. Cosmochim. Acta* 1994, 58, 1701-1710.
41. Stookey, L.L. *Anal. Chem.* 1970, 42, 779-782.
42. Tessier, A.; Campbell, P. G. C.; Bisson, M. *Anal. Chem.* 1979, 51, 844-851.
43. Postma, D. *Geochim. Cosmochim. Acta* 1985, 49, 1023-1033.
44. Stumm, W.; Morgan, J.J. 3<sup>rd</sup> Ed. *Aquatic Chemistry Chemical Equilibria and Rates in Natural Waters*, John-Wiley and Sons, Inc.; New York; 1996.
45. Dzombak, D.A.; Morel, F.M.M. *Surface Complexation Modeling: Hydrous Ferric Oxide*. John Wiley and Sons, Inc.; New York; 1990.
46. Kastler, J.A.; Wilberg, P.L. *Estuar. Coastal Shelf Sci.* 1996, 42, 683-700.